J Eng Math (2008) 60:221–240
DOI 10.1007/s10665-007-9141-y

Free-surface granular flows down heaps

Stuart B. Savage

Received: 20 July 2006 / Accepted: 7 February 2007 / Published online: 28 March 2007

Abstract The present paper extends the granular-flow constitutive model of Savage (1998 J Fluid Mech 377:1–26) to treat spherical particles. Savage accounted for both quasi-static and collisional stresses by considering: (i) strain-rate fluctuations embodied in a critical state plasticity model, as well as, (ii) individual particle velocity fluctuations modelled by granular-flow kinetic theory. In the present work, the governing equations of the kinetic theory of Jenkins (1998 In: Hermann HJ, Luding S (eds) Physics of Dry Granular Media. Kluwer Academic pp. 353–370) for identical spherical, smooth, inelastic particles are supplemented with additional quasi-static terms that have forms patterned after the corresponding terms in the equations of Savage for two-dimensional disk-like particles. The resulting equations along with side-wall and free-surface boundary conditions are applied to examine free-surface granular flow down a heap contained between two frictional vertical side walls. Width-averaged equations of motion are integrated to obtain depth profiles of mean velocity, granular temperature, solids fraction and the Savage–Jeffrey parameter. Detailed comparisons are made with particle-tracking experiments. When the gap between the vertical side walls is fairly narrow, good agreement is found between the predicted and the measured profiles of mean velocity and granular temperature.

Keywords Collisional stresses · Constitutive equations · Free-surface granular flow · Kinetic theories · Quasi-static stresses

1 Introduction

Over the past half-century a great deal of effort has been devoted to the development of constitutive equations for granular materials. Nevertheless, to a large degree, the accurate prediction of the flows of these materials over a wide range of shear rates and solids concentrations remains an unresolved problem. Some success has been achieved in modelling two limiting flow regimes: (a) the *quasi-static*, rate-independent, plastic regime which has received extensive attention in the soil-mechanics literature, and (b) the fully dynamic *rapid flow* regime (called the *grain-inertia* regime by Bagnold [1]). Very

S. B. Savage (✉)
Department of Civil Engineering & Applied Mechanics, McGill University, Montreal, QC, Canada H3A 2K6
e-mail: stuart.savage@mcgill.ca

sophisticated and detailed constitutive models have been devised by soil mechanicists to handle slow deformations of high-concentration materials characteristic of the quasi-static granular-flow regime [2–11].

Granular-flow kinetic theories for idealized, dissipative particles have been developed to treat the other extreme regime of rapid flows at low and moderate concentrations [12–16]. The kinetic energy associated with the translational velocity fluctuations is analogous to the definition of the kinetic temperature of a gas at the molecular level. The translational velocity fluctuation is defined as $\boldsymbol{c} = (\boldsymbol{v} - \boldsymbol{u})$, where $\boldsymbol{v}$ is the instantaneous particle velocity, $\boldsymbol{u} = \langle \boldsymbol{v} \rangle$ is the mean transport velocity and the brackets designate an ensemble average. The translational granular temperature is defined as $T = \langle c^2 \rangle / 3$, where $3T/2$ is the specific kinetic energy of the translational velocity fluctuations. These kinetic theories have been based on hard-sphere models previously devised for dense fluids at the molecular level [17,18]. The 'hard particle' assumption is a key element in the granular-flow kinetic theories. In this limit of infinitely stiff particles, the collisional contact times tend to zero, and thus, only binary collisions need to be considered. The particle-collision dynamics can be treated in a straightforward way and the evaluation of the Boltzmann collision integral and the determination of various transport coefficients are difficult, but manageable. When the concentration is high, the particles are softer and the deformation rates are low, as in the quasi-static regime, the particles typically experience multiple contacts that are long lasting rather than identifiable, short term, 'collisions'. One cannot analyze the particle interactions in a straightforward way as in the case of rapid flow. The particle interactions are not limited to binary ones and the constitutive modelling is, of necessity, more empirically based.

While the two limiting flow regimes are of intrinsic interest and importance, there are many industrial and natural geophysical granular flows that occur in an intermediate, transitional flow regime that lies between them. It is particularly difficult to devise constitutive models intended to handle this high concentration, rapid flow regime involving extended interparticle frictional contacts and significant quasi-static stress contributions. For the most part, only ad hoc approaches that, in effect, patch together the results from the two extreme flow regimes have been proposed thus far. Savage [19] suggested that, for the case of a gravity-driven free-surface chute flow, one might represent the total stresses as the linear sum of a rate-independent, dry-friction part plus a rate-dependent 'viscous' part obtained from the high-shear-rate granular-flow kinetic theories. The magnitude of the rate-independent contribution was chosen such that the sum of the two parts satisfied the overall momentum equation perpendicular to the flow direction. More detailed analyses based on this approach were formulated by Johnson and Jackson [20] and Johnson et al. [21]. While reasonable results were obtained for these particular problems, it was not obvious how the approach could be extended to handle more general kinds of flow problems.

Savage [22] pursued a somewhat different approach to develop a microscopic theory for slow, high-concentration flows at low stress levels. It considered stresses resulting from both collisional particle interactions as well as longer-term frictional contacts. To keep things as simple as possible, the grains were considered to be uniform-size rods or disks, rather than physically more realistic three-dimensional particles. Savage introduced strain-rate fluctuations [23] into a critical-state plasticity model that is similar in form to those proposed for quasi-static, pressure-dependent yielding of soils. The root-mean-square values of the strain-rate fluctuations were related to the granular temperature. The forms of various expressions and constants involved in the model were chosen so that the predictions for high deformation rates were consistent with the collisional, granular-flow kinetic theory of Jenkins [15] for disks. At low deformation rates, the apparent form of the constitutive behaviour was similar to that of a liquid in the following sense. The effective viscosity decreased with increasing granular temperature, as opposed to rapid granular flows in which viscosity increases with increasing granular temperature. Savage [22] considered two example flows: (a) an infinite simple shear flow in the absence of gravity, and (b) the flow down a long, rough-walled vertical channel. For simple shear flow, the resulting expressions for stresses were comprised of two parts; a rate-independent part, and a part that has a quadratic dependence on shear rate. Similar Bingham-like expressions have been proposed in the past on a more ad hoc basis. The second analysis that dealt with slow flow down a rough-walled, vertical channel was able to reproduce the observed experimental characteristics

of nearly constant-thickness side-wall boundary layers (of about 10 particle diameters) with plug flow in the centre, regardless of the gap between the vertical side walls. The constitutive modelling in the present work is based on extensions of this previous work of Savage [22].

1.1 Granular surface flow as a prototype spanning all flow regimes

A particularly interesting rheological granular-flow case study is that of a hopper-fed, gravity-driven, free-surface granular flow down a wedge-shaped pile of 'static' granular material. Such a pile can be generated by pouring granular material between two vertical walls on to a rough horizontal rectangular plate that acts as a base between the two vertical walls. The wedge-shaped pile will grow and reach an equilibrium steady state when the free surface corresponds to the angle of repose and the mass-flow rate of granular material past the edge of the horizontal base plate equals the mass-flow rate supplied by the hopper. In the middle region of the inclined upper free surface a steady fully developed flow is established in which the flow-field properties are independent of downstream distance. Near the free surface, the particle motions can be very vigorous such that the flow corresponds to the rapid-flow, grain-inertia regime where the interparticle collisions are nearly instantaneous. Farther down from the free surface, the concentration increases, particles experience longer-term, multiple contacts and the quasi-static stress contributions are significant. Deep into the pile, the deformation rates tend to zero, the concentration tends to limiting values and the stress states correspond to the quasi-static regime or a static state. Thus, in one very simple flow geometry, the flows span the full range from the rapid-flow, grain-inertia regime to the quasi-static regime or even a static state. The velocities decay in an approximately exponential fashion with depth and there is no need to impose a 'bed' boundary condition in theoretical modelling of such flows.

1.2 Recent investigations of granular surface flows

Recently, the problem of surface flow down a heap of granular material as described above has been examined both theoretically and experimentally. A review of dense granular flows in various configurations, including surface flow down heaps and surface flows in rotation drums is contained in [24]. While there are some similarities between the surface flows in rotating drums [25–31] and those down static heaps, the rotating-drum flows exhibit variations in velocity, flow thickness, and surface inclination in the downstream direction that make them of less interest to the present work that deals with fully developed heap flows. Thus, we shall restrict our attention to granular surface flows down static piles in the brief review that follows.

Andreotti and Douady [32] devised a simple theoretical model for surface flows in which spherical grains were assumed to move in layers parallel to the free surface. They accounted for the driving force of gravity, the dissipation due to interparticle collisions, and the trapping of grains between the bumps of the underlying layer of particles. The velocity profiles and flow depths were determined as a function of surface-inclination angle. Khakhar et al. [33] performed a more traditional depth-averaged hydrodynamic-type analysis in which they assumed the shear stresses were composed of a Bagnold-type collisional stress which depended on the square of the shear rate, and a Coulomb frictional stress involving an effective coefficient of dynamic friction. The velocity profile was assumed to be linear. Complementary experiments were performed with steel balls (2 ± 0.2 mm diameter) flowing between vertical transparent PMMA walls spaced 10 mm apart. They measured the maximum free-surface inclination angle β_m and the layer thickness δ, as functions of the mass-flow rate. Some experiments were performed in an open system in which grains exited a hopper into the main container and proceeded to flow out of its downstream end. They also performed experiments in a closed system to determine streamwise variations of layer thickness, but these are not of interest here.

Somewhat earlier, Lemieux and Durian [34] carried out related experimental measurements of the transition from intermittent avalanching flows to continuous granular surface flows. The experiments of Komatsu et al. [35] found that a very slow creeping flow exists deep in the pile below the rapidly flowing surface layer. The mean velocity of the creeping motion decayed exponentially with depth.

Bonamy and Mills [36] proposed that the flows could be separated into two 'phases', a 'solid' phase that experienced slow creeping motions and a more rapidly flowing phase near the upper surface. They formulated a non-local constitutive law and applied it to solve for (a) the surface granular flow down an infinite pile, and (b) steady surface flows in large rotating drums. A linear velocity profile was obtained for the region near the upper surface and a profile that decayed exponentially with depth was found for deeper regions. Bonamy and Mills [36] obtained reasonable agreement between this theory and experiments performed with steel beads in a rotating drum by Bonamy et al. [25].

Taberlet et al. [37] measured the variation of the free-surface inclination with discharge rate for the flow of sand between vertical plates having different spacings. For narrow gaps they observed a strong increase in surface inclination with increasing flow rate. These experiments called attention to the sizeable effects of side-wall friction.

Josserand et al. [38] adopted a phenomenological description of the constitutive behaviour following Savage [19] and Johnson and Jackson [20]. Stresses were assumed to be made up of a collisional Bagnold-like term that depended on concentration and the square of the shear rate, and a quasi-static contribution that depended on solids concentration. One of the problems they analysed, based on this constitutive behaviour, was fully developed surface flow down a static heap. Velocity and solids-concentration profiles were determined. They found a Bagnold-like velocity profile near the free surface, a linear velocity profile somewhat lower down, and an exponentially decaying velocity profile deeper in the pile.

Jop et al. [39] have performed detailed experiments that further elucidated the importance of side-wall friction effects on granular surface flows. In these studies, the free-surface inclination was found to increase with flow rate for a constant gap width W between the vertical side walls, and to increase at a given flow rate with decreasing W. The thickness of the surface flow was found to increase with increasing gap width W. Because of the frictional side walls, the surface velocity profile was found to vary across the width of the flow. Jop et al. [39] proposed an empirical friction law developed from the basal friction model of Pouliquen and Forterre [40]. Jop et al. [39] predicted velocity profiles across the depth by using this friction law and accounting for the effects of sidewall friction. Their model showed that the depth of flow decreased with decreasing gap width W as was observed in their experiments. They noted some discrepancies between the observed and predicted shapes of the velocity profiles. Their model predicted a zero shear rate at the free surface whereas the experiments showed a finite value there. The model also predicted a finite thickness of flow above a static pile of material whereas the observations revealed an exponentially decaying velocity deep into the pile.

1.3 Present investigation

Constitutive equations for the present work are obtained by extending the slow, high-concentration, strain-rate fluctuation theory of Savage [22] for disk-like particles to treat three-dimensional, spherical particles (cf. previous discussion in Sect. 1). The model of Savage [22] attempted to account for both quasi-static and collisional stresses. It was based on the assumption of fluctuations in strain rates [23] as well as individual particle-velocity fluctuations of the kind handled in the granular-flow kinetic theories. The quasi-static contributions arose from the strain-rate fluctuations embodied in the critical-state plasticity model. In the present analysis we shall introduce terms in the governing equations that are intended to account for the effects of the long-term frictional contacts. However, we shall add them in a somewhat more ad hoc fashion than was done in [22]. As a starting point, we make use of the granular-flow kinetic theory of Jenkins [16] for spherical, smooth, inelastic particles. This is assumed to be appropriate to handle rapid

flows at moderate concentrations in the collisional flow regime. We then append to the governing equations of Jenkins [16] the additional quasi-static terms that have forms patterned after the corresponding terms in the equations of Savage [22] for two-dimensional disk-like particles. The resulting equations are thus formulated to handle, in a relatively simple way, flows that range from the slow, quasi-static flow regime to the rapid-flow, collisional, grain-inertia flow regime.

These governing equations are used to examine a simple shear flow. Various flow characteristics are determined as functions of a generalized coefficient of restitution that attempts to account for dissipative processes of a more general kind than those due to normal collisional impacts. Next, the free-surface granular flow down a heap contained between two rough vertical side walls is analysed. Boundary conditions that consider stress, particle velocity, granular temperature and solids fraction at the free surface and at the vertical solid side walls are considered. The equations of motion corresponding to a width-averaged flow are integrated to obtain depth profiles of mean velocity, granular temperature, solids fraction and the Savage–Jeffrey parameter [13]. Detailed comparisons are made with particle-tracking experiments of Jesuthasan [41,42].

2 Governing conservation and constitutive equations

2.1 Granular-flow kinetic theory of Jenkins

We begin by summarizing some results of the granular-flow kinetic theory formulated by Jenkins [16] for identical, spherical, smooth, inelastic particles. The Chapman–Enskog transport equation [43, Sect. 14.4] was used to obtain the equations expressing the conservation of mass, momentum and fluctuation kinetic energy (i.e., the granular-temperature equation) given by

$$\frac{\partial \rho}{\partial t} + \frac{\partial (\rho\, u_i)}{\partial x_i} = 0\,, \tag{1}$$

$$\rho\, \frac{\mathrm{D}u_i}{\mathrm{D}t} = \rho \left(\frac{\partial u_i}{\partial t} + u_j \frac{\partial u_i}{\partial x_j} \right) = \rho g_i - \frac{\partial p_{ij}}{\partial x_j}, \tag{2}$$

$$\frac{3}{2}\, \rho\, \frac{\mathrm{D}T}{\mathrm{D}t} = \frac{3}{2}\, \rho \left(\frac{\partial T}{\partial t} + u_j \frac{\partial T}{\partial x_j} \right) = -p_{ij} \frac{\partial u_i}{\partial x_j} - \frac{\partial q_j}{\partial x_j} - \gamma\,, \tag{3}$$

where $\rho = \nu\, \rho_p$ is the bulk mass density, ν is the solids volume fraction, ρ_p is the mass density of the individual particles, t is time, u_i is the velocity component in the x_i-direction, g_i is the component of the gravitational acceleration in the x_i-direction, p_{ij} is the symmetric pressure tensor, T is the granular temperature, q_i is the flux of particle fluctuation energy in the x_i-direction, and γ is the rate of energy dissipation per unit volume arising from inelastic collisions.

For non-equilibrium flows of dissipative particles, Jenkins assumed the velocity distribution function to be a perturbed Maxwellian. To leading order, most of the constitutive relations are the same as the classical results for a dense fluid comprised of perfectly elastic, smooth, spherical particles as presented in [18, Sect. 16.34]. The only expression that is different is the collisional dissipation term γ that appears in the particle fluctuation energy equation (3). The pressure tensor (in which compressive stress is taken as positive) is given by

$$p_{ij} = (p - \varpi\, e_{kk})\, \delta_{ij} - 2\mu\, e_{ij}\,, \tag{4}$$

where the pressure p is

$$p = \rho\, T\, (1 + 4\, G)\,, \tag{5}$$

and the bulk viscosity ϖ is

$$\varpi = \frac{8}{3\sqrt{\pi}}\,\rho\,\sigma\,T^{1/2}\,G, \tag{6}$$

where σ is the particle diameter. The rate-of-strain tensor is

$$e_{ij} = \frac{1}{2}\left[\frac{\partial u_i}{\partial x_j} + \frac{\partial u_j}{\partial x_i}\right], \tag{7}$$

and

$$G = \nu\, g_0\,, \tag{8}$$

where $g_0(\nu)$ is the radial distribution function. In the present work we shall use the expression proposed by Lun and Savage [14] and subsequently employed by Johnson and Jackson [20] (see also [13,44]), i.e.,

$$g_0(\nu) = \frac{1}{\left[1 - (\nu/\nu_\infty)^{1/3}\right]} \tag{9}$$

in which $\nu_\infty = 0.64$ is the maximum solids fraction at closest packing.

The shear viscosity μ is expressed as

$$\mu = \frac{\sqrt{\pi}}{6}\,\rho\,\sigma\,T^{1/2}\left[1 + \frac{5}{16\,G} + \frac{4\,G}{5}\left(1 + \frac{12}{\pi}\right)\right], \tag{10}$$

and the energy flux vector is

$$q_i = -\kappa\frac{\partial T}{\partial x_i}\,, \tag{11}$$

where the conductivity κ is

$$\kappa = \frac{15\sqrt{\pi}}{16}\,\rho\,\sigma\,T^{1/2}\left[1 + \frac{5}{24\,G} + \frac{6\,G}{5}\left(1 + \frac{32}{9\,\pi}\right)\right]. \tag{12}$$

The collisional rate of energy dissipation per unit volume is given by

$$\gamma = \frac{24\,(1-e)\,\rho\,G\,T}{\sigma}\left[\frac{T}{\pi}\right]^{1/2}, \tag{13}$$

where e is the coefficient of restitution for the particles.

We are concerned here primarily with dense, high-concentration flows in which the solids fraction $\nu > 0.4$. The expressions (5), (10) and (12) for p, μ and κ contain kinetic as well as collisional terms. At high concentration, the kinetic terms are negligible and these expressions can be further approximated and expressed in the forms

$$p = 4\,\rho\,G\,T\,, \tag{14}$$

$$\mu = \frac{2\,\sigma\,p}{5\,(\pi\,T)^{1/2}}\left[1 + \frac{\pi}{12}\right], \tag{15}$$

$$\kappa = \frac{\sigma\,p}{(\pi\,T)^{1/2}}\left[1 + \frac{9\,\pi}{32}\right]. \tag{16}$$

Similarly, the expression (6) for the bulk viscosity ϖ can be rewritten as

$$\varpi = \frac{2\,\sigma\,p}{3\,(\pi\,T)^{1/2}}\,. \tag{17}$$

Finally, Eq. 13 for the collisional rate of energy dissipation per unit volume can be rearranged in the form

$$\gamma = \frac{6\,(1-e)\,p}{\sigma}\left[\frac{T}{\pi}\right]^{1/2}. \tag{18}$$

2.2 Inclusion of quasi-static contributions

The constitutive equations just presented are based on the assumption of instantaneous binary particle collisions. We now modify them in an ad hoc way in an attempt to account for the existence of long-term frictional-rubbing contacts. We shall add quasi-static terms whose forms are chosen by mimicking the corresponding constitutive expressions derived for the two-dimensional strain-rate fluctuation, critical-state plasticity model of Savage [22]. This model was based on the assumption of an elliptical yield function. The centre of the ellipse corresponded to the mean normal stress, a. It was assumed that the yield ellipse grows in size with increases in solids fraction ν and granular temperature T. It was further assumed that $a(\nu, T)$ was composed of the sum of two contributions such that

$$a(\nu, T) = a_\nu(\nu) + a_T(\nu, T)\,, \tag{19}$$

where $a_\nu(\nu)$ is the quasi-static contribution and $a_T(\nu, T)$ is the collisional pressure contribution that in the present case would correspond to the granular-flow kinetic-theory expression (14)

$$a_T(\nu, T) = 4\,\rho\,G\,T\,. \tag{20}$$

The quasi-static contribution was assumed to have the form

$$a_\nu(\nu) = a_0 \log\left[\frac{\nu_\infty - \nu_0}{\nu_\infty - \nu}\right], \tag{21}$$

where a_0 is a reference value of a_ν, ν_∞ is the solids fraction corresponding to closest packing, and ν_0 is the minimum solids fraction. Note that in the present work we shall assume a slightly different alternative form in which there is an explicit cut-off of the quasi-static contribution when the solids fraction is less than a minimum value ν_0, i.e.,

$$\begin{aligned} a_\nu(\nu) &= a_0\left[\frac{\nu - \nu_0}{\nu_\infty - \nu}\right] \quad \text{for } \nu_0 \le \nu \le \nu_\infty\,, \\ a_\nu(\nu) &= 0 \qquad\qquad\qquad\quad \text{for } \nu < \nu_0\,. \end{aligned} \tag{22}$$

The strain-rate fluctuation, critical-state plasticity model of Savage [22] produced expressions for the constitutive formulas for μ, κ and γ that had functional forms similar to Eqs. 10, 12 and 13 obtained from the above kinetic theory. The slight difference was that a, which included both quasi-static and collisional contributions, appeared in μ, κ and γ in place of the mean collisional pressure p that can be factored out of the collisional kinetic theory expressions. In the present analysis we assume that $a_T(\nu, T)$ is equal to the mean pressure p given by (14) and that $a_\nu(\nu)$ is given by (22) analogous to that used previously by Savage [22].

To include quasi-static effects in the present modelling we merely replace the mean pressure p that appears in (4), (15–17) and (18) by

$$a(\nu, T) = a_\nu(\nu) + a_T(\nu, T) = a_0\left[\frac{\nu - \nu_0}{\nu_\infty - \nu}\right] + 4\,\rho\,G\,T\,, \tag{23}$$

which includes both quasi-static and collisional contributions, and $a_\nu(\nu)$ is given by (22). Hence, we can write for the pressure tensor, shear viscosity, bulk viscosity and conductivity

$$p_{ij} = (a - \varpi\, e_{kk})\,\delta_{ij} - 2\mu\, e_{ij}\,, \tag{24}$$

$$\mu = \frac{2\,\sigma\,a}{5\,(\pi\,T)^{1/2}}\left[1 + \frac{\pi}{12}\right], \tag{25}$$

$$\varpi = \frac{2\,\sigma\,a}{3\,(\pi\,T)^{1/2}}\,, \tag{26}$$

$$\kappa = \frac{\sigma\, a}{(T\,\pi)^{1/2}} \left[1 + \frac{9\,\pi}{32}\right]. \tag{27}$$

The expression for the collisional rate of energy dissipation per unit volume can be rearranged in the form

$$\gamma = \frac{6\,(1-e_g)\,a}{\sigma} \left[\frac{T}{\pi}\right]^{1/2}, \tag{28}$$

where we have replaced e, the restitution coefficient for inelastic normal collisions, in (18) by e_g, which we interpret as a generalized restitution coefficient that in a crude empirical way can account for both dissipative normal impacts and the effects of frictional particle interactions. Jenkins' model [16] does not explicitly include energy dissipation due to frictional particle interactions and the use of e_g is a rough attempt to take some account of these effects. Increasing friction would thus correspond to a decrease in e_g and a larger rate of collisional energy dissipation.

3 Simple shear flow

Let us consider the case of a steady-state, simple shear flow in the absence of gravity in which $\partial u_1(x_2)/\partial x_2 = \partial u(y)/\partial y = \text{const.}$, $u_2 = v = 0$ and $u_3 = w = 0$. The continuity equation (1) and the momentum equation (2) are identically satisfied. The granular temperature will be uniform, and the energy equation (3) reduces to a balance between the shear work and the collisional energy dissipation, i.e.,

$$-p_{xy}\frac{\partial u}{\partial y} - \gamma = \mu \left[\frac{\partial u}{\partial y}\right]^2 - \gamma = 0\,. \tag{29}$$

Substituting (25) and (28) for μ and γ in (29) we obtain

$$\frac{\sigma^2}{T}\left[\frac{\mathrm{d}u}{\mathrm{d}y}\right]^2 = R^2 = \frac{15\,(1-e_g)}{(1+\pi/12)}, \tag{30}$$

where $R = \sigma\,(\mathrm{d}u/\mathrm{d}y)/\sqrt{T}$ is the so-called Savage–Jeffrey [13] parameter. Figure 1 shows a plot of R versus the generalized restitution coefficient e_g.

By making use of (24) and (25) we can express the shear stress as

$$-p_{xy} = 2\,\mu\,e_{xy} = \mu\,\frac{\partial u}{\partial y} = \frac{2\,\sigma\,a}{5\,(\pi\,T)^{1/2}}\,(1+\pi/12)\,\frac{\partial u}{\partial y}\,. \tag{31}$$

Finally, by making use of (23) and (30), the shear stress can be written as

$$-p_{xy} = \frac{2\,\sigma}{5\,\pi^{1/2}}\,(1+\pi/12)\left[a_0\left[\frac{\nu-\nu_0}{\nu_\infty-\nu}\right] + \frac{4\,\rho\,G\,\sigma^2}{R^2}\left[\frac{\partial u}{\partial y}\right]^2\right]. \tag{32}$$

This has the form of an extended Bingham-type fluid with a power-law dependence on shear rate that has previously been proposed to describe the behaviour of granular materials [45–49]. For a particular solids fraction ν, the first term on the right-hand side of (32) is a constant term that is independent of shear rate and the second term depends on the square of the shear rate as in the classical paper of Bagnold [1]. The x- and y-components of the pressure tensor are equal and given by (24) as

$$p_{xx} = p_{yy} = a \tag{33}$$

in which a is composed of a rate-independent term and a term that depends on the square of the shear rate. The ratio of shear to normal stress is equal to the ratio of the components of the pressure tensor $|p_{xy}/p_{yy}|$. It is independent of solids fraction and the shear rate and is given by

$$\left|\frac{p_{xy}}{p_{yy}}\right| = \left[\frac{12\,(1-e_g)\,(1+\pi/12)}{5\,\pi}\right]^{1/2}. \tag{34}$$

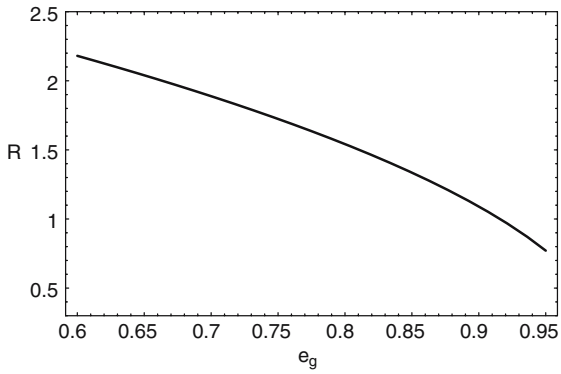

Fig. 1 Variation of the Savage–Jeffrey parameter R with the generalized restitution coefficient e_g for the case of simple shear flow

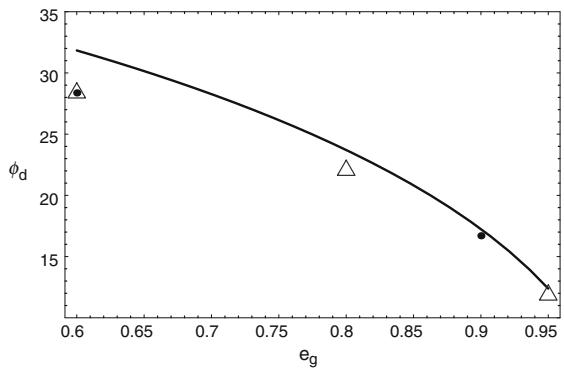

Fig. 2 Variation of dynamic friction angle ϕ_d (degrees) with the generalized restitution coefficient e_g for the case of simple shear flow. Comparison of present theory (solid line) given by (34) with computer simulations of Hopkins and Shen [50] (filled circles) and Lun and Bent [51] (open triangles)

We can define a dynamic friction angle $\phi_d = \arctan |p_{xy}/p_{yy}|$. Figure 2 shows the dynamic friction angle ϕ_d determined from (34) and plotted as a function of the generalized restitution coefficient e_g. Also shown in Fig. 2 are results of the Molecular Dynamics and Monte Carlo simple shear flow simulations of Hopkins and Shen [50] and the Molecular Dynamics simulations of Lun and Bent [51], both of which are consistent with similar calculations of Walton and Braun [52]. The simulations are for the case of frictionless particles such that $e_g \to e$, and the plotted values correspond to a solids fraction $\nu = 0.5$. The kinetic-theory result given by (34) is very close to the simulations for high e, but departs somewhat from them as e is decreased. The kinetic-theory analysis is, in effect, a small-parameter expansion for small inelasticity $(1 - e)$ and it is expected to become inaccurate as $(1 - e)$ increases.

4 Analysis of granular surface flow down a heap

Let us consider the free-surface granular flow down a heap as shown in Fig. 3 where x is the streamwise coordinate aligned parallel to the upper surface that is inclined at an angle θ to the horizontal, y is the coordinate perpendicular to the free surface and oriented in the downward direction into the pile, and z is oriented perpendicular to the x–y plane of the figure. The flow is assumed to take place between two vertical side walls that are perpendicular to the z-direction and spaced a distance b apart. The side walls are frictional and can have a significant effect on the flow, but the gap b is taken to be sufficiently small such that we can neglect the z-variations of certain flow properties. Thus, we shall approximate the flow as steady, fully developed, and two-dimensional, and solve the conservation equations for the y-distributions of the velocity u in the streamwise x-direction, the solids fraction ν, and granular temperature T.

4.1 Governing equations for steady, fully developed flow

Since we assume a steady, fully developed flow, there are no variations of flow quantities in the x-direction, i.e., $\partial/\partial x = 0$ and the mean velocity components in the y and z-directions vanish; thus, $v = 0$ and $w = 0$. We further assume that the transverse z-variations of streamwise velocity u, granular temperature T, and solids fraction ν are small. The governing conservation equations eventually can be reduced to ordinary

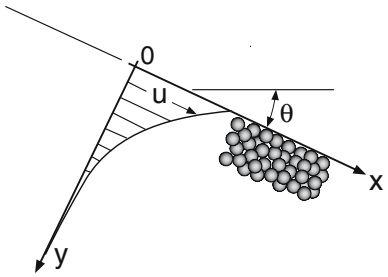

Fig. 3 Diagram of free-surface granular flow down a heap

differential equations that only involve variations with the y-coordinate. Note that the continuity equation (1) is identically satisfied. The x and y-components of the linear momentum equation (2) can be expressed as

$$\rho \frac{\mathrm{D}u}{\mathrm{D}t} = 0 = \rho g \sin\theta - \frac{\partial p_{xy}}{\partial y} - \frac{\partial p_{xz}}{\partial z}, \tag{35}$$

$$\rho \frac{\mathrm{D}v}{\mathrm{D}t} = 0 = \rho g \cos\theta - \frac{\partial p_{yy}}{\partial y}, \tag{36}$$

and the fluctuation energy equation (3) reduces to

$$\frac{3}{2}\rho \frac{\mathrm{D}T}{\mathrm{D}t} = 0 = -p_{xy}\frac{\partial u}{\partial y} - \frac{\partial q_y}{\partial y} - \frac{\partial q_z}{\partial z} - \gamma\,. \tag{37}$$

The mean velocity of the particles at the frictional side walls is directed in the x-direction, so that pressure tensor components $p_{xz} = p_{zx}$ can develop. But, we assume that there is no wall shear stress acting in the y-direction and hence, in writing (36) we have taken $p_{yz} = p_{zy} = 0$. The right-hand side of (37) was obtained by assuming that $\partial u/\partial z \simeq 0$. We make the approximation that p_{xz} and q_z vary linearly across the width z such that

$$p_{xz} = p_{xz}^0\,(1 - 2\,z/b) \quad \text{and} \quad q_z = q_z^0\,(1 - 2\,z/b)\,, \tag{38}$$

where p_{xz}^0 and q_z^0 correspond, respectively, to the shear stress and fluctuation energy flux at the side wall, $z = 0$. Hence, we can express $\partial p_{xz}/\partial z$ and $\partial q_z/\partial z$ that, respectively, appear in (35) and (37) as follows

$$\frac{\partial p_{xz}}{\partial z} = -\frac{2}{b}\,p_{xz}^0 \quad \text{and} \quad \frac{\partial q_z}{\partial z} = -\frac{2}{b}\,q_z^0\,, \tag{39}$$

where expressions for p_{xz}^0 and q_z^0 will be determined in the following subsection by consideration of the boundary conditions at the vertical side walls.

4.2 Boundary conditions

In order to completely specify the governing equations (35–39), and to subsequently carry out their integration from the upper surface down into the pile, we must define boundary conditions both at the upper surface and at the vertical side walls.

4.2.1 Upper-surface boundary conditions

We begin by considering the boundary conditions at the upper surface of the flow. It is convenient to divide the flow vertically into two regions; a lower region that encompasses most of the particulate domain, and an upper surface region that comprises one, or in some cases, a few layers of particles. Both the flux of fluctuation energy and the particle stress should vanish at the upper surface. If we view the region occupied

by the granular material as a continuum, then the solids fraction near the surface tends to zero sharply or even discontinuously. If the particles are packed together as a plug flow, such that the granular temperature is zero, then the free surface can be unambiguously defined. For the usual instances, where there are more vigorous interactions between particles that give rise to a significant granular temperature, the treatment of the boundary conditions at the free surface is less distinct, particularly when one considers matters on the individual-particle scale.

The treatment of the free-surface boundary conditions has been examined by Johnson et al. [21]. They first considered the case of more moderate granular temperatures near the free surface and took account of the discrete nature of the particulate material. Johnson et al. [21] considered a force balance for a particle in the layer adjacent to the upper free surface. The components of the weight of a particle in the uppermost layer were equated to the associated shear and normal forces that can be deemed to act on an underlying plane area parallel to the upper surface, i.e.,

$$\frac{\pi}{6}\,\rho_p\,\sigma^3\,g_i = p_{ij}\,n_j\,a_c\,, \tag{40}$$

where a_c is the area associated with the individual particle, p_{ij} is the stress acting on a_c at the top of the underlying layer just beneath the particle, and n_j is the inward directed unit normal. Following Bagnold [1], the average distance between particles was defined as s and the solids fraction was expressed as

$$\nu = \nu_\infty \left[\frac{\sigma}{\sigma + s}\right]^3\,, \tag{41}$$

such that $\nu \to \nu_\infty$ as $s \to 0$. Thus, the area a_c associated with one particle in the top layer was expressed as

$$a_c = \sigma^2 \left[\frac{\nu_\infty}{\nu}\right]^{2/3}\,. \tag{42}$$

In the case of more rapid flows, where there are more vigorous particle interactions, a dilute saltating region can develop at the upper surface.

In the present analysis we shall assume that the normal stress p_{yy} that appears in (40) is purely collisional and given by (14). This enables us to obtain an expression for the granular temperature T_1 one particle diameter below the 'free surface'. Thus, from (40) and (42) we find

$$T_1 = \frac{\pi}{24}\,\frac{\sigma\,g\,\cos\theta}{\nu_1\,G_1}\left[\frac{\nu_1}{\nu_\infty}\right]^{2/3}\,, \tag{43}$$

where ν_1 and G_1 correspond respectively to values of the solids fraction and G one particle diameter below the 'free surface'.

4.2.2 Side-wall boundary conditions

We next consider the boundary conditions for the shear stress and the fluctuation energy flux at the vertical solid side walls by following an approach similar to that of Johnson et al. [21]. The mean velocity of the particles adjacent to the side wall is in the x-direction and the shear stress developed by the wall acts in the negative x-direction so as to resist the motion. We relate the side wall shear stress to the normal stress acting perpendicular to the wall through the use of a wall friction angle δ. Thus, we can express p^0_{xz} at the wall, $z = 0$ as

$$p^0_{xz} = -\,p^0_{zz}\,\tan\delta = -\,p^0_{yy}\,\tan\delta = -\,p_{yy}\,\tan\delta = -\,a\,\tan\delta \tag{44}$$

since we approximate $p_{zz} = p_{yy} = a$ as being independent of z.

Johnson et al. [21] considered the energy balance for a small volume that enclosed an element of the solid boundary and derived the condition

$$\boldsymbol{n}\cdot\boldsymbol{q}^0 = -\mathcal{D} - \boldsymbol{u}^0\cdot\boldsymbol{S}^0_c\,, \tag{45}$$

where $\boldsymbol{n}$ is the unit normal to the wall directed into the granular material, $\boldsymbol{q}^0$ is the particle fluctuation energy flux at the wall, $\mathcal{D}$ is the rate of energy dissipation due to inelastic collisions with the wall, $\boldsymbol{u}^0$ is the particle mean slip velocity at the wall and $\boldsymbol{S}^0_c$ is the collisional force per unit area at the wall. Note that the first term $-\mathcal{D}$ on the right-hand side of (45) is negative and gives rise to a reduction of the granular temperature, whereas the last term $-\boldsymbol{u}^0\cdot\boldsymbol{S}^0_c$ is positive and corresponds to a production of granular temperature. We assume that the wall-slip velocity $\boldsymbol{u}^0$ is approximately equal to the mean streamwise velocity u and that the collisional shear stress at the wall is given by the product of the collisional normal pressure, $a_T = 4\,\rho\,G\,T$, and the wall friction coefficient, $\tan\delta$. Thus, we can rewrite (45) as

$$q^0_z = -\mathcal{D} + u\,a_T\,\tan\delta = -\mathcal{D} + 4\,\rho\,G\,T\,u\,\tan\delta\,. \tag{46}$$

Following Johnson et al. [21] and Nott and Jackson [53] we express the wall collisional energy dissipation $\mathcal{D}$ as

$$\mathcal{D} = \frac{\sqrt{3}\,\pi\,\rho_p\,(\nu/\nu_\infty)\,(1-e_w^2)\,T^{3/2}}{4\left[1-(\nu/\nu_\infty)^{1/3}\right]}\,, \tag{47}$$

where e_w is the coefficient of restitution between the particles and the side wall.

4.3 Reduced form of governing equations

By making use of the approximations (38), the boundary conditions given by (44), (46) and (47), we can rearrange the governing equations (35–37) in the form of the coupled system of ordinary differential equations as follows

$$\frac{\mathrm{d}p_{xy}}{\mathrm{d}y} = \rho g\,\sin\theta - \frac{2\,p_{yy}}{b}\,\tan\delta\,, \tag{48}$$

$$\frac{\mathrm{d}p_{yy}}{\mathrm{d}y} = \rho g\,\cos\theta\,, \tag{49}$$

$$\frac{\mathrm{d}}{\mathrm{d}y}\left[\kappa w\frac{\mathrm{d}w}{\mathrm{d}y}\right] + \frac{1}{2\,\mu}\,p^2_{xy} - \frac{\gamma}{2} + \frac{1}{b}\,q^0_z = 0\,, \tag{50}$$

where $w(y) = T^{1/2}$, and from (25), (27), and (28) with $a = p_{yy}$, we can write

$$\mu = \frac{2\,\sigma\,p_{yy}}{5\,\sqrt{\pi}\,w}\left[1+\frac{\pi}{12}\right], \tag{51}$$

$$w\,\kappa = \frac{\sigma\,p_{yy}}{\sqrt{\pi}}\left[1+\frac{9\,\pi}{32}\right], \tag{52}$$

$$\gamma = \frac{6\,(1-e_g)\,p_{yy}\,w}{\sigma\,\sqrt{\pi}}\,. \tag{53}$$

From the definition of the shear stress given by (24) we obtain an equation for the velocity profile

$$\frac{\mathrm{d}u}{\mathrm{d}y} = -\,\frac{1}{\mu}\,p_{xy}\,, \tag{54}$$

and from (23) we obtain an expression that can be used to solve for the solids-fraction distribution, i.e.,

$$a = p_{yy} = a_0\left[\frac{\nu-\nu_0}{\nu_\infty-\nu}\right] + \frac{4\,\rho_p\,\nu^2\,w^2}{\left[1-(\nu/\nu_\infty)^{1/3}\right]}\,. \tag{55}$$

4.4 Integration of governing equations

We now describe the approximate approaches used to integrate the governing equations and obtain the profiles of mean velocity, granular temperature, the Savage–Jeffrey parameter, solids fraction and related flow variables. Note that in an actual physical situation, such as the experiments of Jesuthasan [41,42], the mass-flow rate is fixed at the outlet of the supply hopper. Thus, the surface flow inclination angle, mean velocity u, granular temperature T, and solids fraction ν develop so as to be consistent with a steady fully developed flow. Hence, the flow field is established as a function of the flow rate. In our calculations, the flow rate is inversely connected to the flow field as follows. We specify a value for the granular temperature at the upper layer and proceed to calculate the profiles of T, u and ν from which we could subsequently determine the mass-flow rate.

We first consider Eqs. (48) and (49) and approximate the mass density ρ that appears in these equations by a mean density $\overline{\rho} = \rho_p\, \overline{\nu}$ over the depth of flow under consideration. We then integrate (49) over y from the position just below the top layer of particles where the normal stress is given by $p_{yy}^{(1)} = 4\,\rho_p\,\nu_1\,G_1\,T_1$. Thus, we find

$$p_{yy} = p_{yy}^{(1)} + \overline{\rho}\, g\, \cos\theta\, y\,, \tag{56}$$

where as implied above, the origin of the y-coordinate is taken to be one particle diameter below the upper surface. Integrating (48) in a similar way we obtain

$$p_{xy} = p_{yy}^{(1)}\, \tan\theta + \overline{\rho}\, g\, \cos\theta\, y - \frac{2\,\tan\delta}{b}\left[p_{yy}^{(1)}\, y + \overline{\rho}\, g\, \cos\theta\, \frac{y^2}{2}\right]. \tag{57}$$

We next solve (50) in an iterative fashion. Let us begin by neglecting the last term, q_z^0/b, on the left-hand side of (50). What remains in (50) is an ordinary differential equation for $w(y)$ involving p_{yy} and p_{xy} that have just been determined. Using the `NDSolve` routine contained in the software system *Mathematica* 5.0, Eq. 50 can be integrated numerically over y starting with trial value of $w = w_1 = T_1^{1/2}$. We then determine the mean velocity u from (54) and (51) such that $u \to 0$ at large depths. Then, the previously determined values of w, u, and the assumed mean value of $\overline{\rho}$ are used to determine q_z^0 from (46) and (47). This relation for q_z^0 is used in (50) which is again numerically integrated using the `NDSolve` routine to determine w as a function of y. The mean velocity u is recalculated with the revised expression for w. Finally, by using (55) and the expressions for p_{yy} and w, it is possible to determine the variation of ν with depth y.

4.5 Numerical results and comparisons with experimental measurements of Jesuthasan

4.5.1 Jesuthasan's particle-tracking experiments on free-surface granular flows

Jesuthasan [41,42] has performed digital particle-tracking velocimetry (DPTV) measurements of a free-surface granular flow down a wedge-shaped pile of 'static' granular material. The granular flow took place between two vertical glass walls that were spaced a distance b apart. The tests involved a series of spacings of $b = 25.4$, 38.1 and 50.8 mm, and for each spacing, three mass-flow rates were tested. The three nominal mass-flow rates per unit width $\dot{m}/b$ were 0.81, 1.85 and 3.33 $\mathrm{kg\,s^{-1}\,m^{-1}}$. The test particles were nearly uniform, spherical ceramic (zirconium silicate) beads having a mean effective diameter of 1.59 mm and mass density of, 4,071 $\mathrm{kg/m^3}$. Digital images of the granular flows in the fully developed region were obtained by a high speed digital camera system. The commercial PTV software package `DiaTrackPro 2.3` was used along with especially written *Matlab* routines to obtain the particle trajectories and profiles of mean velocity, granular temperature, and the Savage–Jeffrey parameter at the glass side wall.

Table 1 Values of particle and channel wall properties used in calculations

Quantity	Symbol	Value
Particle diameter	σ	1.59 mm
Particle mass density	ρ_s	4071 kg/m^3
Maximum solids fraction	ν_∞	0.64
Minimum frictional solids fraction	ν_0	0.50
Wall friction angle	δ	14°
Particle coefficient of restitution	e_g	0.86
Wall coefficient of restitution	e_w	0.8

Table 2 Values of width between side walls b, surface inclination angle θ, and mass flow per unit width $\dot{m}/b$, in various test runs of Jesuthasan [41]

Test run	b	θ	$\dot{m}/b$ (kg s^{-1} m^{-1})
AA	$16\,\sigma$	20.9°	0.78
AC	$16\,\sigma$	23.5°	3.29
BC	$24\,\sigma$	22.8°	3.38
CC	$32\,\sigma$	21.7°	3.33

4.5.2 Comparison of theoretical predictions with the experiments of Jesuthasan

The previous section Sect. 4.4 discussed the procedures used to integrate the governing differential equations. Here we present the results of the numerical integrations to determine the profiles of the mean streamwise velocity u, the granular temperature T, the solids fraction ν, the Savage–Jeffrey parameter R, the collisional contributions to the normal pressure, and the total normal pressure. The predicted profiles of u, T and R are compared with the corresponding experimental profiles measured by Jesuthasan [41] in four representative test runs.

Tables 1 and 2 show the values of various particle and channel wall properties and flow geometries associated with the calculations and the experiments. The values of the particle diameter σ and mass density ρ_p, the wall friction angle δ, the width between the side walls b (in particle diameters σ), the free-surface inclination angle θ, and the mass-flow rate per unit width $\dot{m}/b$ correspond to those measured in the experiments. The remaining quantities ν_∞, ν_0, e_g and e_w are assumed values that are thought to be reasonable. They were not chosen or adjusted to achieve better fits of the theory to the experiments of Jesuthasan [41].

Run AA. Figure 4(a–g) show the results of the calculations for run AA of [41] having values for the channel width b, and surface inclination angle θ, as specified in Table 2. The value of $w_1 = T_1^{1/2}$, at one particle diameter from the upper surface, was chosen to approximate the experimentally measured value. No particular effort was taken to optimize the fit between the theoretically predicted and experimentally measured mean velocities and granular temperatures, and it is possible that better agreement could be obtained by fine-tuning the value of w_1. Figure 4(a) shows good agreement between the predicted mean velocity u and the experimental measurements of [41] for run AA. The predicted velocity is plotted using semi-log coordinate scales in Fig. 4(b). The fact that the curve of velocity is nearly a straight line indicates that the velocity exhibits an almost exponential decay with depth. Figure 4(c) shows reasonably good agreement between the predicted and measured granular-temperature profiles. Figure 4(d) shows the predicted variation of solids fraction ν with depth y. Near the upper free surface, the particles are loosely packed, but further down the solids fraction is close to the maximum packing value ν_∞. Figure 4(e) shows the predicted and measured variation of the Savage–Jeffrey parameter R with depth y. Both the mean velocity u and the granular temperature T are quite small for depths $y > 0.01$ m. Hence, the experimentally determined value of R, which depends on the ratio of the velocity gradient $\mathrm{d}u/\mathrm{d}y$ and the square root of the granular temperature T, is subject to some uncertainty and scatter. Nevertheless, the analysis predicts

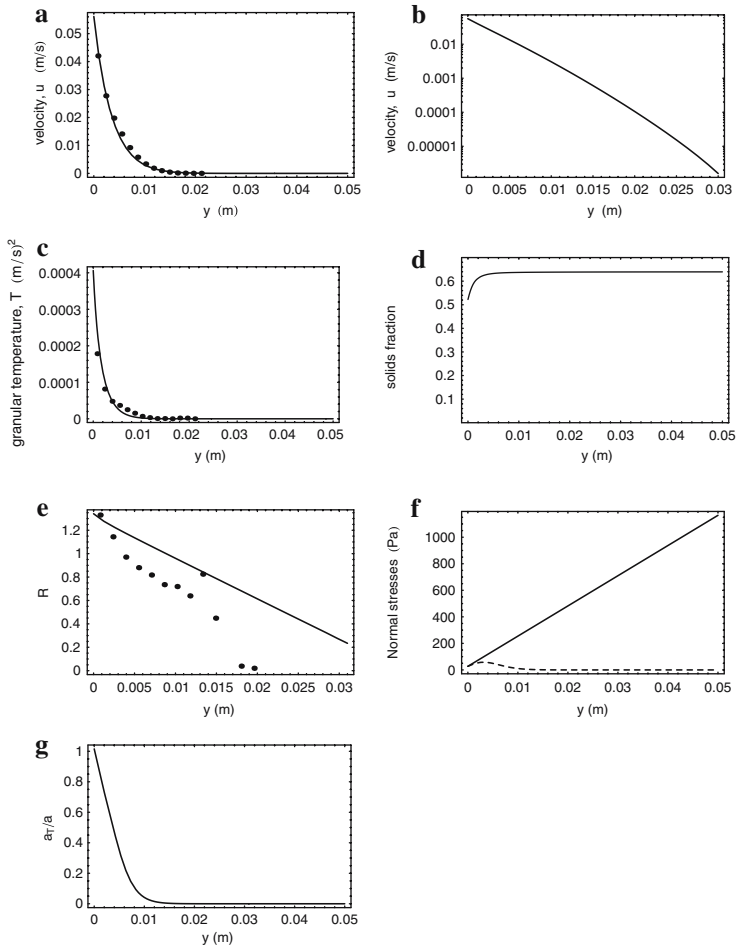

Fig. 4 Variation of flow quantities with depth y. Predictions compared with data from experiment AA of Jesuthasan [41] in (**a**), (**c**) and (**e**). (**a**) streamwise mean velocity u, (**b**) streamwise mean velocity u, (**c**) granular temperature T, (**d**) solids fraction ν, (**e**) Savage–Jeffrey parameter R, (**f**) a_T (dash line); total pressure a (solid line), (**g**) ratio a_T/a

the proper trend of R versus y. Note that because of the side-wall friction, R decreases with depth. An approximation that has been used previously (for example, see the discussion in [54]) has been to assume in the granular-temperature energy equation, that there is a balance between the shear work term and the collisional energy dissipation. This assumption would yield a constant value for R over the depth. We also find that if the flow is assumed to be two-dimensional, and wall friction is neglected, then the present governing equations again will yield a constant value of R over the depth of the flow. Figure 4(f) shows the variation of the total normal pressure $a = p_{yy}$ with depth (indicated by a solid line), and the depthwise variation of a_T, the collisional contribution to the pressure, (indicated by a dashed line). Figure 4(g) shows the ratio of a_T/a plotted as a function of depth y. Near the upper free surface, the pressure is due almost entirely to interparticle collisions, but as the depth increases, the quasi-static contribution becomes more important, and at large depths the pressure p_{yy} arises essentially from the quasi-static effects.

Run AC. Similar calculations were performed for run AC of Jesuthasan [41] and some results are shown in Fig. 5(a–d). In going from run AA to run AC, the mass-flow rate per unit width $\dot{m}/b$ was increased by a factor of about 4.2 and the corresponding free-surface inclination angle θ increased from 20.9° to 23.5°. The depth of flow remained much the same in these two runs. But, at a given depth, the mean velocity u was larger in run AC than in run AA by a factor of roughly 4.2. There is reasonable agreement between

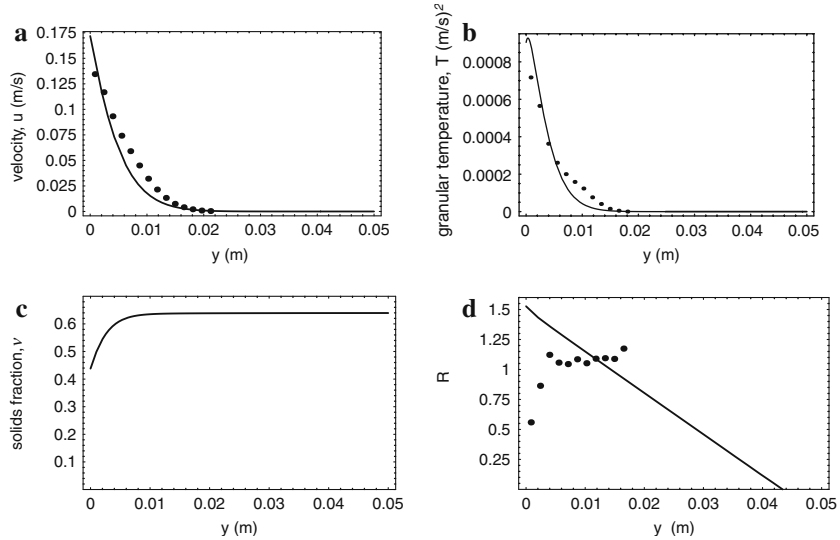

Fig. 5 Variation of flow quantities with depth y. Predictions compared with data from experiment AC of Jesuthasan [41] in (**a**), (**b**) and (**d**). (**a**) streamwise mean velocity u, (**b**) granular temperature T, (**c**) solids fraction ν, (**d**) Savage–Jeffrey parameter R

the predicted and measured profiles of u and T. The experimental values of R are in the same range as the predicted values, but as in the previous case AA, the measurements are scattered. The remaining calculations for run AC were found to have characteristics similar to the corresponding ones for run AA, but for the sake of brevity they are not presented here.

Run BC. Results of calculations corresponding to the experimental run BC of Jesuthasan [41] are shown in Fig. 6(a–d). Run BC involved the same nominal flow rate per unit width $\dot{m}/b$ as for run AC, but the channel width was increased from 16σ to 24σ, with a corresponding decrease in the free-surface inclination angle from 23.5° to 22.8°. There is reasonably good agreement between the experimental and predicted profiles for u and T. The agreement between the experimental and predicted R profile is not as good, but, for the most part, the trends are similar. Figure 7 compares the experimental u velocity profiles for runs BC and AC. The measured wall velocities for run BC are slightly smaller than those for run AC despite the fact that the nominal mass-flow rates per unit width were the same for both runs. Hence, one can infer that the velocities in the center of the channel for run BC were somewhat larger than those measured at the wall.

Run CC. Fig. 8(a–d) show results of calculations corresponding to the experimental run CC of Jesuthasan [41]. Run CC involved the same nominal flow rate per unit width $\dot{m}/b$ as for run AC and BC, but the channel width was increased from 24σ to 32σ with a corresponding decrease in the free-surface inclination angle from 22.8° to 21.7°. For this run, the agreement between the experimental and predicted profiles for u and T is not as good as in the previous comparisons for runs AA, AC and BC. Run CC involves the largest channel width. Based on the evidence noted in the previous subsection, it is expected that the mean velocity and granular temperature varied to some degree across the channel width. These variations were not accurately accounted for in the theoretical analysis. Figure 9 compares the measured velocity profiles for runs BC ($b = 24\sigma$) and CC ($b = 32\sigma$). For the wider channel, the flow depth is larger and the surface velocity is smaller. This same kind of effect of channel width on the flow was observed in the experiments of Jop et al. [39]. Some preliminary exploratory calculations were performed with lower values of the wall friction angle in a crude attempt to model the flows in the central region of the channel away from the frictional side walls. The effect was to increase the depth of the flowing region and to modify the shape of the velocity profiles to look more like the observations. The experimental values

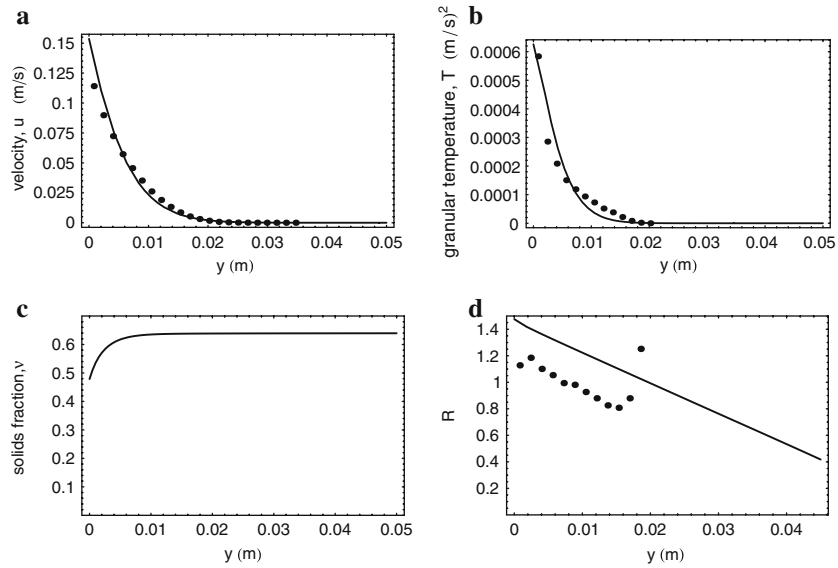

Fig. 6 Variation of flow quantities with depth y. Predictions compared with data from experiment BC of Jesuthasan [41] in (**a**), (**b**) and (**d**). (**a**) streamwise mean velocity u, (**b**) granular temperature T, (**c**) solids fraction ν, (**d**) Savage–Jeffrey parameter R

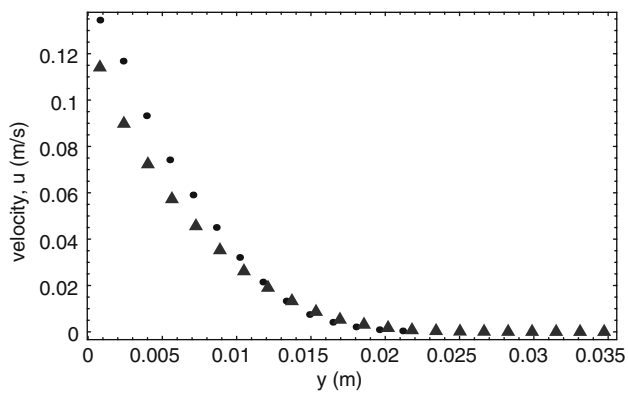

Fig. 7 Comparison of streamwise mean velocity profiles for Jesuthasan's [41] runs AC (circle data points) and BC (triangles)

of R are somewhat below the predicted values (see Fig. 8(d)). Again, the width averaged granular-flow analysis is probably responsible in part for the inaccuracies. It would be worthwhile to perform a full three-dimensional flow analysis in an attempt to accurately predict the flows in the wider channels.

5 Concluding remarks

1. The present work has delineated a theory intended to model granular flows that range from the high concentration, quasi-static flow regime to the moderate and high concentration, collisional, rapid flow regime. It can be regarded as an extension of the slow, high concentration, strain-rate fluctuation theory of Savage [22] for disk-like particles. We began with the granular-flow kinetic theory of Jenkins [16] for identical spherical, smooth, inelastic particles that is capable of handling the rapid flow, collisional regime and appended to it quasi-static terms that have forms patterned after the corresponding terms in the equations of Savage [22].

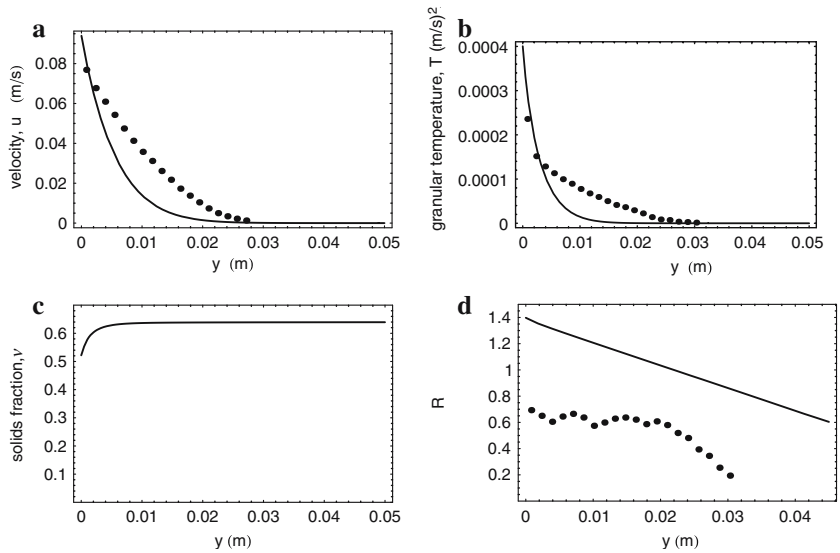

Fig. 8 Variation of flow quantities with depth y. Predictions compared with data from experiment CC of Jesuthasan [41] in (**a**), (**b**) and (**d**). (**a**) streamwise mean velocity u, (**b**) granular temperature T, (**c**) solids fraction ν, (**d**) Savage–Jeffrey parameter R

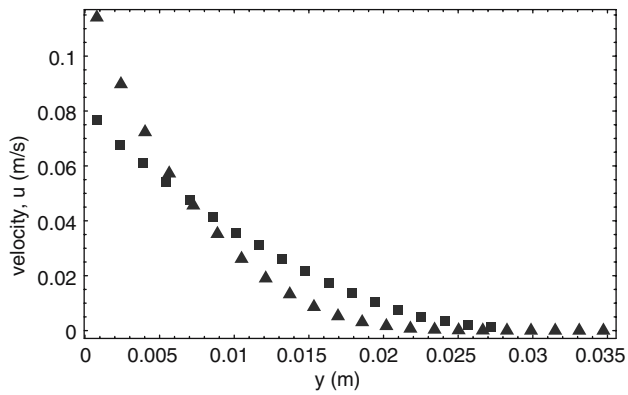

Fig. 9 Comparison of streamwise mean velocity profiles for Jesuthasan's [41] runs BC (triangle data points) and CC (squares)

2. The resulting theory was applied to examine free-surface granular flow down a heap contained between two rough vertical side walls. This is a particularly interesting rheological case study since, in one very simple flow geometry, the behaviour of the granular flow spans the full range from the rapid flow, grain-inertia regime near the upper surface to the quasi-static regime or even a static state deep into the pile. Boundary conditions that involve particle velocity, stress, granular temperature and solids fraction both at the upper free surface and at the vertical, frictional side walls were considered. The existence of the frictional side walls will lead to three-dimensional flow fields. However, the present work was restricted to the case of relatively narrow gaps between the vertical side walls such that some variables could be averaged over the width, thereby reducing the problem to a two-dimensional flow. The resulting equations of motion were integrated to obtain depth profiles of mean velocity, granular temperature, solids fraction and the Savage–Jeffrey parameter.
3. Detailed comparisons were made with particle-tracking experiments of Jesuthasan [41]. When the gap between the vertical side walls is fairly narrow, good agreement was found between predicted profiles of the mean velocities and granular temperatures, and those measured by Jesuthasan [41]. The comparisons for the widest gap were not as good. This is probably due to the existence of variations of mean

velocity and granular temperature across the channel width that were not accurately accounted for in the theoretical analysis.

4. The predictions of the Savage–Jeffrey parameter R were also compared with the experimental values measured by Jesuthasan [41]. It is difficult to accurately determine the experimental values of R and the results presented show some scatter. One approximation that has been proposed for the solution of the granular-temperature equation (cf. [54]) is to assume that there is a balance between the shear work term and the collisional energy dissipation and to neglect the other terms in the fluctuation energy equation. This assumption would yield a constant value for R over the depth. In the present work it was found that R was not constant; it decayed with depth due to the presence of side-wall friction. Thus, some care is advised in using the above mentioned approximation for the energy equation.
5. Further calculations of three-dimensional granular flows for wide channels are worthwhile. The experiments of Jop et al. [39] revealed that the depth of the flowing region increased and the upper-surface velocity decreased when the width of the channel was increased. The experiments of Jesuthasan [41] involved much narrower channels than those of Jop et al. [39], but these same trends were evident.

Acknowledgements This work was sponsored by the Climate Change Action Plan (CCAP) 2000 and a Natural Sciences and Engineering Research Council (NSERC) Discovery Grant. I am grateful to Professor R. Baliga for continuing collaboration during this research program and to Dr. M. Sayed for useful comments and suggestions concerning this paper. I would particularly like to thank N. Jesuthasan for providing me with the details and tabulated results of his free-surface granular-flow experiments.

References

1. Bagnold RA (1954) Experiments on a gravity free dispersion of large solid spheres in a Newtonian fluid under shear. Proc R Soc London A 225:49–63
2. Bolzon G, Schrefler BA, Zienkiewicz OC (1996) Elastoplastic soil constitutive laws generalized to partially saturated states. Géotechn 46:279–289
3. Chen WF, Mizuno E (1990) Nonlinear analysis in soil mechanics. Elsevier, Amsterdam
4. Lade PV, Prabucki M-J (1995) Softening and preshearing effects in sand. Soils Foundations, Japanese Geotechn Soc 35(4):93–104
5. Lade PV, Pradel D (1990) Instability and plastic flow of soils. I: Experimental observations. J Engrg Mech, ASCE 116(11):2532–2550
6. Mroz Z, Norris VA, Zienkiewicz OC (1979) Application of an anisotropic hardening model in the analysis of elasto-plastic deformation of soils. Géotechn 29:1–34
7. Oda M, Nemat-Nasser S, Konishi J (1985) Stress-induced anisotropy in granular masses. Soils Foundations 25:85–97
8. Pradel D, Lade PV (1990) Instability and plastic flow of soils. II: Analytical investigation. J Engrg Mech, ASCE 116(11):2551–2566
9. Vardoulakis IG, Sulem J (1985) Bifurcation analysis in geomechanics. Chapman & Hall, London
10. Vermeer PA (1984) A five-constant model unifying well established concepts. In: Gudehus G, Darve F, Vardoulakis I (eds) Constitutive relations for soils, A. A. Balkema, pp 175–197
11. Wood DM (1990) Soil behaviour and critical state soil mechanics. Cambridge University Press
12. Jenkins JT, Savage SB (1983) A theory for the rapid flow of identical, smooth, nearly elastic particles. J Fluid Mech 130:186–202
13. Lun CKK, Savage SB, Jeffrey DJ, Chepurniy N (1984) Kinetic theories for granular flow: inelastic particles in Couette flow and slightly inelastic particles in a general flowfield. J Fluid Mech 140:223–256
14. Lun CKK, Savage SB (1987) A simple kinetic theory for granular flow of rough, inelastic spherical particles. Trans ASME E: J Appl Mech 54:47–53
15. Jenkins JT (1987) Balance laws and constitutive relations for rapid flows of granular materials. In: Chandra J, Srivastav R (eds) Constitutive models of deformations, SIAM, Philadelphia, pp 109–119
16. Jenkins JT (1998) Kinetic theory for nearly elastic spheres. In: Hermann HJ, Luding S (eds) Physics of dry granular media, Kluwer Academic, NATO ASI Series E: Applied Sciences – vol 350, pp 353–370
17. Cole GHA (1967) The statistical theory of classical simple dense fluids. Pergamon Press, Oxford
18. Chapman S, Cowling TG (1970) The mathematical theory of non-uniform gases, 3rd edn. Cambridge University Press
19. Savage SB (1983) Granular flows down rough inclines - review and extension. In Jenkins JT, Satake M (eds) Mech. of granular materials: new models and constitutive relations. Elsevier, pp 261–82

20. Johnson PC, Jackson R (1987) Frictional-collisional constitutive relations for granular materials, with application to plane shearing. J Fluid Mech 176:67–93
21. Johnson PC, Nott P, Jackson R (1990) Frictional-collisional equations of motion for particulate flows and their application to chutes. J Fluid Mech 210:501–535
22. Savage SB (1998) Analysis of slow high-concentration flows of granular materials. J Fluid Mech 377:1–26
23. Hibler WD III (1977) A viscous sea ice law as a stochastic average of plasticity. J Geophys Res 82:3932–3938
24. GDR MiDi (2004) On dense granular flows. Eur Phys J, E 14:341–365
25. Bonamy DF, Daviaud F, Laurent L (2002) Experimental study of granular surface flows via a fast camera: a continuous description. Phys Fluids 14(5):1666–1673
26. Bonamy DF, Daviaud F, Laurent L, Bonetti M, Bouchaud JP (2000) Multiscale clustering in granular surface flows. Phys Rev Lett 89(3):034301-1–034301-4
27. Hill KM, Gioia G, Tota VV (2003) Structure and kinematics in dense free-surface granular flow. Phys Rev Lett 91(6):064302-1–064302-4
28. Jain N, Ottino JM, Lueptow RM (2002) An experimental study of the flowing granular layer in a rotating tumbler. Phys Fluids 14(2):572–582
29. Khakhar V, McCarthy JJ, Shinbrot T, Ottino JM (1997) Transverse flow and mixing of granular materials in a rotating cylinder. Phys Fluids 9:31–43
30. Khakhar DV, Orpe AV, Ottino JM (2001) Surface granular flows: two related examples. Adv Comp Syst 4:407–417
31. Yamane K, Nakagawa M, Altobelli SA, Tanaka T, Tsuji Y (1998) Steady particulate flows in a horizontal rotating cylinder. Phys Fluids 10:1419–1427
32. Andreotti B, Douady S (2001) Selection of velocity profile and flow depth in granular flows. Phys Rev E 63:031305, 1–8
33. Khakhar DV, Orpe AV, Andersen P, Ottino JM (2001) Surface flow of granular materials: model and experiments in heap formation. J Fluid Mech 441:255–264
34. Lemieux PA, Durian DJ (2000) From avalanches to fluid flow: A continuous picture of grain dynamics down a heap. Phys Rev Lett 85:4273–4276
35. Komatsu TS, Inagaki S, Nakagawa N, Nasumo S (2001) Creep motion in a granular pile exhibiting steady surface flow. Phys Rev Lett 86:1757–1760
36. Bonamy D, Mills P (2003) Diaphasic non-local model for granular surface flows. Europhys Lett 63(1):42–48
37. Taberlet N, Richard P, Valance A, Delannay R, Losert W, Pasini JM, Jenkins JT (2003) Super stable granular heap in thin channel. Phys Rev Lett 91:264301
38. Josserand C, Lagrée P-Y, Lhuillier D (2004) Stationary shear flows of dense granular materials: a tentative continuum modelling. Eur Phys J, E 14:127–135
39. Jop P, Forterre Y, Pouliquen O (2005) Crucial role of side walls for granular surface flows: consequences for the rheology. J Fluid Mech 541:167–192
40. Pouliquen O, Forterre Y (2002) Friction law for dense granular flows: application to the motion of a mass down a rough inclined plane. J Fluid Mech 453:133–151
41. Jesuthasan N (2005) Optical measurements of a free surface granular flow. M Eng Thesis, Dept Mech Engrg, McGill University, Montreal, August 2005
42. Jesuthasan N, Baliga R, Savage SB (2006) Use of particle tracking velocimetry for measurements of granular flows: review and application. KONA 24:15–26
43. Reif F (1965) Fundamentals of statistical and thermal physics. McGraw–Hill, New York
44. Carnahan NF, Starling KE (1969) Equations of state for non-attracting rigid spheres. J Chem Phys 51:635–636
45. Savage SB (1979) Gravity flow of cohesionless granular materials in chutes and channels. J Fluid Mech 92:53–96
46. Takahashi T (1981) Debris flow. Annu Rev Fluid Mech 13:57–77
47. Takahashi T (1991) Debris Flow. A.A. Balkema, Rotterdam
48. Tsubaki T, Hashimoto H (1983) Interparticle stresses and characteristics of debris flows. J Hydrosc Hydr Engrg 1:67–82
49. Chen CL (1988) Generalized visco-plastic modelling of debris flow. J Hydr Engrg, ASCE, 114:237–258
50. Hopkins MA, Shen HH (1992) A Monte Carlo solution for rapidly shearing granular flows based on the kinetic theory of dense gases. J Fluid Mech 244:477–491
51. Lun CKK, Bent AA (1994) Numerical simulation of inelastic frictional spheres in simple shear flow. J Fluid Mech 258:335–353
52. Walton OR, Braun RL (1986) Stress calculations for assemblies of inelastic spheres in uniform flow. Acta Mech 63:73–86
53. Nott P, Jackson R (1992) Frictional-collisional equations of motion for granular materials and their application to flow in aerated chutes. J Fluid Mech 241:125–144
54. van Wachem BGM, Schouten JC, van den Bleek CM, Krishna R, Sinclair J (2001) Comparative analysis of CFD models of dense gas-solid systems. AIChE J 47:1035–1051